Tissue-Engineered Submillimeter-Diameter Vascular Grafts for Free Flap Survival in Rat Model

Hiroki Yamanaka[1, 2], Tetsuji Yamaoka[1*], Atsushi Mahara[1], Naoki Morimoto[3] and Shigehiko Suzuki[2].

[1]Department of Biomedical Engineering, National Cerebral and Cardiovascular Center Research Institute, Suita, Osaka, Japan
[2]Department of Plastic and Reconstructive Surgery, Graduate School of Medicine and Faculty of Medicine, Kyoto University, Kyoto, Japan
[3]Department of Plastic and Reconstructive Surgery, Kansai Medical University, Hirakata, Osaka, Japan

***Correspondence:** Dr. Tetsuji Yamaoka, Department of Biomedical Engineering, National Cerebral and Cardiovascular Center Research Institute, 5-7-1 Fujishirodai, Suita, Osaka 565-8565, Japan.
Tel: +81-06-6833-5012 (Ext: 2637) Fax: +81-06-6835-5476.
E-mail: yamtet@ncvc.go.jp

Abstract

Vascular grafts for free flap transfers should be of very small diameter and remain patent for approximately three weeks to supply blood until the revascularization from the surrounding tissue is established, with the autologous vein grafts acting as the gold standard. Artificial submillimeter-diameter vascular grafts with clinically useful size of 0.6 mm inner diameter and 5 cm length were prepared and evaluated by replacing the axial artery of free flap in rats. The rat tail artery, selected as a novel bioscaffold material, was decellularized using ultrahigh-hydrostatic pressure (UHP) method and compared with the detergent-based conventional method. To induce rapid endothelialization, the graft lumen was modified with synthesized peptides, having high affinity to the endothelial progenitor cells. The UHP method and peptide modification at 37 °C were found to preserve the extracellular matrix structure well, leading to the stable immobilization of the peptide at the luminal surface. These grafts showed the neointima formation, even at the center position far from the native vessels, remained patent for three weeks, and resulted in the flap survival in the rat free-flap model. The tissue-engineered vascular grafts with functionalized lumen have great future potential as an alternative to autologous vein grafts in free flap transfers.

Key words: Free flap, Submillimeter-diameter vascular graft, Acellular, Tissue engineering

1. Introduction

Advances in surgical microscopes, surgical instruments, and anastomosis techniques have made it possible to anastomose smaller-diameter vessels, making submillimeter-diameter vascular anastomoses commonplace for surgeons nowadays. Consequently, various types of microsurgical free flap transfers have been reported and performed for reconstruction of tissue defects caused by tumor resection or trauma. Autologous veins with inner diameter (ID) between 0.5 mm to 2.0 mm are often used to extend the vascular pedicle of the flap and allow them to reach the intact donor vessels. Many series with primary autologous vein grafts in free flap transfers have been reported with satisfactory results [1-4]. However, there are some limitations in using autologous vein grafts [5, 6], such as, the requirement of longer time to harvest the graft, the difficulty to choose the proper vein in diameter, donor site scars, and limited sources. Particularly, one of the most serious problems is that some patients have no available vein because of their prior removal for cosmetic or surgical indications [7], or because of severe peripheral vascular diseases. For instance, the incidence of absent or hypoplastic great saphenous vein is reported more than 30% in limbs with varicosities [8]. Furthermore, it may be better to preserve the great saphenous vein for future life-saving procedures such as coronary artery bypass grafting [6]. Therefore, vascular grafts with IDs smaller than 2 mm acting as alternative to autologous vein grafts are required. In addition, since autonomization of free flaps in humans has been classically considered as approximately three weeks, these vascular grafts for the elongation of flap pedicle should remain patent for at least three weeks [6].

Although synthetic vascular grafts have demonstrated satisfactory long-term results when used in large-diameter arteries, these grafts with IDs smaller than 4 mm are of limited use because of short-term thrombosis [9, 10]. One of the disadvantages of the synthetic vascular grafts is their lack of endothelial cells on the graft lumen, leading to the adherence of the blood proteins and the activation of clotting mechanisms [11]. Most previous animal studies using expanded polytetrafluoroethylene (ePTFE) grafts for the elongation of flap pedicle exhibited negative results because of thrombosis [5, 6, 12-15]. Only one study using 1-mm short grafts to rabbit epigastric flap resulted good patency rates with

flap survival [16]. However, other studies using grafts longer than 5 cm could not achieve even few-weeks patency required for flap survival [6, 14]. Moreover, synthetic materials such as ePTFE or polyethylene-terephthalate fiber (Dacron™) have another great disadvantage related to the lack of remodeling, thus eliminating any potential for growth or vasoreactivity [17]. The tissue defects requiring free flap transfers often have poor blood flow and synthetic materials are prone to infection.

Given these limitations of the synthetic vascular grafts, biodegradable tissue-engineered vascular grafts (TEVGs) have great possibility of being an ideal alternative to autologous vein grafts. Various approaches to vascular tissue-engineering have been proposed, which can be divided into two groups: scaffold-based method with or without cell-seeding and self-assembly using cell-sheets technology [9]. The acellularization may be important for producing the off-the-shelf vascular grafts since culturing autologous cells is time-consuming; hence, various groups have focused on acellular TEVGs. Some acellular TEVGs such as SynerGraft™ [18] and Omniflow-II™ [19] have shown enough progress to be readily available for human use. However, since functional endothelium is necessary to maintain graft patency [20], methods to capture cells after implantation are required particularly in acellular TEVGs with smaller IDs. To address this, we previously succeeded in modifying the luminal surface of decellularized vessels with synthesized peptides, which have high affinity to endothelial progenitor cells (EPCs) [21]. The ostrich carotid arteries decellularized by the ultrahigh hydrostatic pressure (UHP) treatment followed by washing and modification with the peptides demonstrated the rapid *in vivo* re-endothelialization and good short-term patency in a porcine femoral-femoral bypass model. This approach has two key points for future success in microsurgical TEVGs, namely, biodegradability, which is a general feature of decellularized tissue, and the neointima-inducing activity without the need for seeding of the autologous cells.

In this study, we present an acellular submillimeter-diameter vascular graft with the functionalized lumen, which can be used to replace or extend the vascular pedicle of free flap using the rat tail artery as the novel scaffold material for the vascular tissue-engineering. The graft size with 0.6 mm in inner diameter

and 5 cm in length is suitable for microsurgery. Previously reported submillimeter-diameter TEVGs were less than 1-cm length in animal experiments [22, 23]; this is the first report of acellular micro-vascular grafts with clinically useful length. We prepared four groups, including three different conditions in peptide modification for the UHP method and the conventional detergent-based decellularization method. The denaturation of extracellular matrix (ECM) structures during decellularization or peptide-modification process and the stability of the peptides on graft lumen were analyzed. Graft transplantations were carried out in the high responder ACI-to-Lewis rat model; the vascular grafts prepared from ACI rats were transplanted to the epigastric flaps of Lewis rats. The primary endpoint is the flap survival with patent axial artery replaced with the vascular grafts at the period of three weeks.

2. Materials and Methods

2.1. Decellularization of the graft

Tail arteries were harvested from ACI rats (between 200 g and 220 g, Japan SLC, Inc., Hamamatsu, Japan). The ACI rats were anesthetized with inhalation isoflurane and oxygen. A silicon tube was applied on the base of the tail as a tourniquet and ventral skin of the tail was resected. After the fascia was dissected, the tail artery was explored. Then, the dorsal branches of the tail artery were ligated and the tail artery was isolated (Fig. 1A). After washing out with heparinized saline solution by using 24-gauge catheters, arteries were divided into two groups and were decellularized with the UHP method or a conventional detergent-based method using sodium dodecyl sulfate (SDS).

In the UHP group, arteries were decellularized as described previously [21, 24, 25]. The arteries were pressurized at 1,000 MPa for 10 min using Dr. Chef high-pressure food processor (Kobe Steel, Ltd., Kobe, Japan). It took 15 min each for the pressure to increase to the target value and then to decrease to the atmospheric pressure. After the UHP treatment, the sample was immersed in saline containing 40 U/mL of DNase I (Roche Applied Science, Indianapolis, IN, USA), 20 mM $MgCl_2$, and antibiotics for 1 day under 37 °C. The sample was then washed with saline containing 500 mg/L of EDTA and antibiotics to remove the

remaining DNase I and Mg^{2+} and was stored in the same solution at 4 °C.

The other arteries were decellularized with the detergent-based method by using the following steps: first, they were immersed in 1 wt.% SDS for 6 h, then washed with deionized water for 1 h, then immersed in 1 wt.% *t*-octylphenoxypolyethoxy-ethanol (Triton X-100) for 1 h, and finally washed with PBS for 1 h under 37 °C. The quality of decellularization of each method was histologically evaluated with H&E stains. The amount of remaining DNA was also checked using a DNeasy Blood & Tissue Kit (Qiagen, Inc., Hilden, Germany) and fluorescence DNA quantification kit (Bio-Rad Laboratories, Inc., Hercules, CA, USA) (n=3).

2.2. Peptide modification

The synthesized peptides, having the sequences $(Pro\text{-}Hyp\text{-}Gly)_7$-Gly-Gly-Gly-Arg-Glu-Asp-Val (POG7G3REDV) [21], were purchased from Sigma-Aldrich Japan (Tokyo, Japan). The $(Pro\text{-}Hyp\text{-}Gly)_7$ sequence has been reported to bind the collagen fiber [26]. The luminal surface of the decellularized graft was modified with the peptides just before transplantation. We prepared four groups of peptide-modified grafts as follows. First, the decellularized grafts of the UHP group were divided into three groups and incubated in 10 μM peptide solution in saline at each condition: at 60 °C for 1 h and cooled to room temperature (RT) (UHP-60), at 37 °C for 1 h and cooled to RT (UHP-37), and at 4 °C for 24 h (UHP-4). Second, the grafts decellularized with SDS were incubated in the same peptide solution at 37 °C for 1 h and cooled to RT (SDS-37). After peptide modification, these grafts were washed with saline before experimental usage. The luminal surface of each graft and that of the native tail artery as the control were observed with scanning electron microscopy (SEM) to evaluate the structural change of the extracellular matrix (ECM) caused by protein denaturation after both decellularization and peptide-modification process. In addition, to analyze the adverse effect of ECM denaturation, biomechanical property of each graft was investigated. Each graft and the native artery of 1.5-cm length were connected to a closed circuit respectively. The circuit was filled with PBS and pressurized in 10-mmHg steps up to 200 mmHg while outer diameter of the graft was measured. Then relative

change in outer diameter with pressurization was compared in each group.

Alexa Fluor 633-labeled POG7G3REDV peptides were used to examine the stability of peptides binded to collagen at the graft lumen. Alexa Fluor 633 NHS esters (Thermo Fisher Scientific Inc., Waltham, MA, USA) were added to the peptide solution and incubated for 3 h at the RT. The labeled peptides were purified with the PD-10 column. Using the labeled peptide, four groups of grafts described above were also prepared. Then, each graft was interposed to the tail artery of Lewis rat (300–400 g, Japan SLC, Inc., Hamamatsu, Japan) under heparinization and was removed after the perfusion for 1 h. We evaluated *in vivo* stability of the immobilized peptides by comparing the fluorescence intensity of the graft lumen before and after the perfusion, using confocal laser scanning microscopy.

2.3. Transplantation of the graft

Lewis rats of 8 weeks weighing 200–250 g (Japan SLC, Inc.) were used as the recipients. First, we examined whether the survival of the epigastric flap, the standard experimental flap model [27], depended on the blood flow from the pedicle. After that, transplantations of acellular grafts to free flaps were carried out.

2.3.1. Rat free flap model

In six rats, each left epigastric flap was raised as described previously [28]. After the induction of anesthesia with inhalation of isofulurane and oxygen, the abdomen and the groin were shaved, and the left epigastric flap of 2 cm square was designed. Under a surgical microscope, the femoral vessels were ligated distal to the origin of the epigastric vessels, and the ramifications of the left femoral vessels were ligated except for the epigastric vessels, then the flap was raised completely based on the left femoral vessels (Fig. 2A). Three flaps were sutured back into the original part with the pedicle ligated, while the other three flaps were left with the pedicle remaining intact. After 3 days, blood flow of the flap was evaluated with gross appearance and laser speckle contrast imaging (moorFLPI-1, Zero C Seven, Inc., Tokyo, Japan).

2.3.2. Transplantation of acellular blood vessels to the artery of the flap

A total of 18 grafts were transplanted to Lewis rats as follows: 6 grafts (UHP-60), 6 grafts (UHP-37), 3 grafts (UHP-4) and 3 grafts (SDS-37). Anesthesia was induced with 2.5% isoflurane and maintained by mask inhalation of 1.5–2.5% isoflurane. The left epigastric flap of 2 cm square was raised as described above. After systematic administration of 200 IU/kg heparin, the left femoral artery feeding the flap was ligated proximal to the origin of the epigastric artery. Another incision of 2 cm was made at the right groin, and the right femoral artery was isolated. Each graft with 5-cm length was transplanted into the subcutaneous tunnel between the right and left femoral artery to reperfuse the flap (Fig. 3). Each anastomosis was performed in an end-to-end fashion by 6–8 interrupted sutures using 10/0 nylon (Microsurgery suture DU-3mm, Kono Seisakusho, Co., Ltd., Tokyo, Japan) with disposable micro-vascular double clip (TKF-2-15, BEAR Medic Corporation, Tokyo, Japan). After the anastomoses were completed, the clamps were released, and flap reperfusion was assessed with moorFLPI-1. An immediate patency of the graft was checked by the milking test and the laser doppler flowmetry (Omega Flow FLO-C1, Omega wave, Tokyo, Japan). Finally, the flap was replaced to the origin and surgical wounds were closured with 3/0 silk interrupted sutures. To prevent bleeding from the anastomotic site because of heparinization, each rat was kept in rest under anesthesia for 3 h after heparin administration.

After 1, 7, and 21 days, the graft patency was checked with ultrasonic diagnosis (Prosound II, SSD-6500 SV, Hitachi Aloka Medical, Ltd., Tokyo, Japan), and blood flow of the flap was assessed with moorFLPI-1. When the blood flow of the graft was unclear in the Doppler color image, the graft was checked directly. At the 21st day, all patent grafts were extracted, and rats were sacrificed. After washing with heparinized saline, the endothelialization of grafts was histologically evaluated with CD31 immunostains and the formation of thrombosis or aneurysm was evaluated with H&E stains. For CD31 immunostaining, fresh samples were embedded in Tissue-Tek O.C.T. compound (Thermo Fisher Scientific, Waltham, MA, USA) and were frozen with liquid nitrogen. Sections of 8 μm were cut and stained as follows: the sections were first dehydrated with ethanol, then immersed in hydrogen peroxide diluted in

methanol, washed with TBST, incubated with Dako Protein Block (X0909, Dako, Glostrup, Denmark) at RT for 5 min, incubated with primary antibodies (550300, BD Biosciences, San Jose, CA, USA) at 4 °C overnight, washed with TBST, incubated with Simple Stain Rat (Nichirei Biosciences, Inc, Tokyo, Japan) at RT for 30 min, washed with TBST, incubated with DAB chromogen (K3468, Dako) for 5 min, and finally counterstained with hematoxylin. The H&E staining protocol was as follows: tissue sections of 8 μm were dipped in deionized water for 3 min, incubated in hematoxylin for 10 min, rinsed under running tap water for 15 min, incubated in eosin for 2 min, rinsed in DW for several times, dehydrated with ethanol, and finally lucidificated with xylene.

2.3.3 Ethic statements

All animal experiments were conducted in accordance with the guidelines for animal experiments established by the Ministry of Health, Labor and Welfare of Japan, and by the National Cerebral and Cardiovascular Center Research Institute, Japan. The protocol was approved by the Committee on the Ethics of Animal Experiments of the National Cerebral and Cardiovascular Center Research Institute (Permit Number: 17043).

3. Results

In this study, four types of grafts were compared in removal of cells, retaining of the native ECM structures, biomechanical property, stability of collagen-binded peptides, and *in vivo* experiment in rat free-flap model.

3.1. Properties of acellular grafts

Cell removal by each decellularization method was confirmed by H&E staining (Fig. 4A). There was no visible nuclear material after decellularization by UHP or SDS method. The amount of remaining DNA was less than 50 ng per mg of the material in either method (Fig. 4B). The luminal surface of each graft and that of the native tail artery were observed with the SEM (Fig. 5A). The endothelial cells, observed on the luminal surface of the native artery, were completely peeled off from the luminal surfaces of all decellularized grafts. In the UHP groups, the luminal ECM structures appeared different depending on the

temperature of the peptide modification. Expectedly, the ECM structures of the grafts treated at 60 °C were severely denatured like frizz across the whole area. On the other hand, only partial denaturation was observed in the grafts treated at 37 °C and 4 °C. The ECM structures of SDS-37 appeared wavy and more disrupted than those of the UHP group treated with the same temperature during peptide-modification process. Interestingly, these appearances of the ECM structures were strongly correlated with the alterations of biomechanical properties of the vascular grafts (Fig. 6). UHP-60 showed more stiffness and SDS-37 was more compliant than the native artery. Although the UHP treatment made the vascular grafts stiff, UHP-37 and UHP-4 showed minimal alterations of the biomechanical properties.

We evaluated the stability of the peptides immobilized on the luminal surface of each group by comparing the fluorescence intensity before and after in situ perfusion using the fluorescence-labeled peptide (Fig. 5B). Before perfusion, the fluorescence intensities of luminal surface were high in all groups. In UHP-60 and UHP-37, the fluorescent intensities were maintained even after perfusion for 1 h, while that in UHP-4 was drastically decreased. The intensity was also decreased in SDS-37.

3.2. Rat free flap model

We verified that the survival of the epigastric flap sized 2 cm square depended on the blood flow from the pedicle (Fig. 2B). After 3 days, all three flaps with the pedicle remaining intact were demonstrated to be vital with normal skin color and positive blood flow of moorFLPI-1 (Fig. 2B a). In contrast, all three flaps with the pedicle ligated had negative blood flow and showed total necrosis with eschar (Fig. 2B b).

3.3. Acellular graft transplantation

Each graft was transplanted to connect the epigastric flap of Lewis rat to the contralateral femoral artery, while the flap venous drainage remained intact. First, in the two groups with well-stabilized peptides (UHP-60 and UHP-37), six grafts per each group were transplanted. As controls, three grafts were transplanted for each of the other two groups (UHP-4 and SDS-37).

With the almost similar ID between the decellularized graft and the recipient vessel (0.6 mm and 0.7 mm, respectively), the end-to-end anastomoses were carried out without need to correct the diameter difference. The results of transplantations are summarized in Table 1. All rats survived for 3 weeks and there was no evidence of hind limb ischemia. Immediate patency was achieved in all grafts. All six grafts of UHP-60, which had well-stabilized peptides but were little stiffer than the other grafts, were occluded in 3 weeks, while they were patent at 7 days. On the other hand, all six grafts of UHP-37, which had well-stabilized peptides and showed almost normal compliance, were patent at 3 weeks. This difference of patency rates was statistically significant ($p = 0.0022$, Fisher's exact test). In the UHP-4 group, two of three grafts were patent at 3 weeks. In the SDS-37 group, all three grafts were occluded in 3 weeks. In a total of 18 flaps, 16 flaps survived with good hair growth and were demonstrated to be vital with good blood flow measured with moorFLPI-1 (Supplemental Figure S1). One case in the UHP-37 group showed partial flap loss due to self-mutilation and one in the SDS-37 group showed total flap necrosis on day 7 because of the graft occlusion on day 1.

The endothelialization of each patent graft was histologically evaluated with CD31 immunostains (Fig. 7A). The likely endothelial-cell migration from the native arteries to the transplanted grafts was observed over 1 mm from the suture line in all patent grafts. Intriguingly, in UHP-37, CD31 positive cells were found lining on the luminal surface even at the position distant from the suture line, but were not observed in UHP-4. Some patent grafts were partially bulging, and these lesions were demonstrated to be the minor dissecting aneurysms (Fig. 7B). Platelet aggregations were also observed around the lesion.

Discussion

Recently, decellularized tissues are attracting great attention not only for their similarity to the native tissues but also for various biological functions [29-31]. A number of clinical products based on the decellularized tissues are now available for various applications, such as reconstruction of musculoskeletal tissue, cardiovascular structures, lower urinary tract, gastrointestinal tract, and central nervous system [32]. In vascular tissue-engineering, various tissues of

animal origin such as the carotid artery [21, 33], the mesenteric vein [34], the ureter [35], and the small intestinal submucosa [36] have been reported as the scaffold materials. A product based on the decellularized human veins has also been developed (SynerGraft^{TM}) [18]. However, these grafts have IDs larger than 2 mm and are not suitable for microsurgical usage. In this study, we focused on the rat tail artery, which has submillimeter diameter and length of longer than 5 cm, as novel bioscaffold material of vascular grafts. As the result, we succeeded for the first time in achieving flap survival by transplanting acellular micro-vascular grafts of clinically useful length to the arterial defects of free flaps.

We have reported that *in vivo* recellularization of acellular vascular graft can be achieved by luminal surface modification to recruit EPCs [21]. The luminal surface modification exploits the strong affinity of the collagen mimetic peptides (CMPs) of sequence -(Pro-Hyp-Gly)$_n$- to natural collagen [26]. The mechanism of CMP binding to natural collagen was investigated in detail by using synthesizing CMP- conjugated gold nanoparticles [37] or fluorescence-labeled CMPs [38]. Major points are as follows:

1. The melting of CMPs into monomers is necessary for the stabilization onto collagen and the incubation temperature should be above the melting temperature (Tm) of the CMPs.
2. Moderate heat creates additional reactive sites in collagen by partial denaturation and increases the CMP binding.
3. Extensive heat leads to severe denaturation of collagen and reduces the CMP binding.

Given these characteristics of CMP binding to natural collagen, the incubation temperature during the peptide modification should be between the Tm of POG7G3REDV (about 37 °C, unpublished data) and that of collagen fiber (65.1 °C [39]). In our previous work, the decellularized ostrich carotid arteries demonstrated good short-term patency by combining with peptide modification at 60 °C, close to the Tm of collagen fiber, determined for the purpose of increasing the peptide binding. However, in our preliminary experiments, rat tail arteries treated with similar conditions did not patent even for two weeks. One plausible reason is the adverse effect of ECM denaturation caused by heating to 60 °C during peptide immobilization. In thliis study, therefore, we prepared three

groups with different incubation temperatures (UHP-60, UHP-37 and UHP-4) and investigated the relationship between the ECM denaturation, peptide binding, and patency rate. As a result, heating to 60 °C led to good stability of peptides but highly denatured ECM and poor patency. The moderate heating to 37 °C succeeded in stabilizing the peptides on the luminal surface while preserving the natural ECM structures and led to good patency with endothelialization. The fluorescence-labeled peptides treated at 4 °C were washed out even by short perfusion period and endothelialization was not observed in UHP-4. These observations corroborate our previous report that peptide modification contributes to rapid endothelialization on the luminal surface. In addition, we decellularized the other group by the conventional method using the chemical detergents. The ECM denaturation observed in SDS-37 might be due to decellularization process, since peptide-modification under 37 °C did not denature the luminal ECM structures in UHP-37. The decellularized grafts with highly denatured ECM could not achieve three-week patency (UHP-60 and SDS-37), while the grafts with well-preserved ECM showed good patency rates (UHP-37 and UHP-4). It is well established that a compliance mismatch between the graft and the native vessel produces medium- to long-term intimal hyperplasia and subsequent stenosis [17, 40]. However, particularly in a low flow state, such as our microsurgical study, it is not surprising that the compliance mismatch causes disturbed flow or turbulence, decreased distal perfusion, and subsequent short-term thrombosis [40]. In other words, maintaining the native ECM structures is one of the most important key points in decellularized small-diameter vascular tissue-engineering.

The decellularization process is the compromise between removing antigenic cellular material and maintaining the ECM [29]. The cell remnants resulting from inadequate decellularization cause adverse immune reactions, whereas aggressive treatment may remove and/or denature even the important ECM components, leading to altered mechanical properties of the material. Although the chemical detergents such as SDS have been generally used to decellularize various tissues, it has been suggested that residual chemicals have cytotoxicity and may inhibit *in vivo* recellularization of decellularized tissues [10]. The UHP treatment can eliminate such risks of chemical detergents and lead to more

effective removal of cell components than detergent-based decellularization [24, 25]. Moreover, the UHP treatment suppresses the virus activity [21] and does not require terminal sterilization processes, such as ethylene oxide exposure, gamma irradiation, and electron beam irradiation, which are known to alter ECM ultrastructure and mechanical properties.

Aneurysm formation is one of the common disappointing outcomes of acellular vascular grafts, but may be prevented by adding cells onto graft lumen [10]. However, TEVGs by cell-seeding or self-assembly are not suitable for the usage in emergency surgeries since they can lead to longer period of time for culture of the autologous cells. Theoretically, luminal surface modification of decellularized grafts to promote rapid *in vivo* endothelialization has a possibility to prevent aneurysm formation as well as cell-seeding before transplantation. In this study, however, we could not prove the hypothesis as aneurysm formation was observed even in UHP-37, in which re-endothelialization was observed. One possible reason is the excessive tension to the graft after transplant surgery because of the hyperactivity of the hip joint or rapid growth of the rat; this is a limitation of the rat model.

There are other limitations in this study. First, there is absence of long-term follow up in this study. The primary reason is that a reliable ‘short-term’ patency of vascular grafts is sufficient for flap survival, since free flap is revascularized from the surrounding tissue within three weeks after the transplantation. However, for longer and clinical usage, the incidence of graft rupture should be preferably investigated. We did not observe clear rapture of the ostrich carotid artery-derived acellular vascular grafts in minipigs [21] and goats (unpublished data). However, since the rat tail artery derived acellular grafts have very fragile and thinner graft walls, it is of prime importance to study its biodegradation property and the recellularization process of the middle layer under long-term transplantation model. Second, the thrombogenicity mechanisms of animals are not similar to humans [41]. The thrombogenic specificity of rats might lead to decellularized grafts of UHP-4 to patent despite the absence of endothelial layer formation. Further investigations using large animal model with comparable thrombogenicity mechanisms are required.

In conclusion, this is the first report of submillimeter-diameter TEVGs for free

flap transfers. These grafts have clinically useful length, 5 cm. The micro-vascular grafts, decellularized by UHP treatment and modified at 37 °C, showed good short-term patency with re-endothelialization. Although there are still some limitations, such as aneurysm formation and absence of long-term follow up, the tissue-engineered acellular vascular grafts with functionalized lumen have great future potential as an alternative to autologous vein grafts in free flap transfers.

Acknowledgments

The authors thank Dr. Koko Asakura, Ph.D. (Department of Data Science, National Cerebral and Cardiovascular Center, Japan) for valuable comments on the statistical analysis. This research was partially supported by the Japan Agency for Medical Research and Development (AMED) Sinnovation-Program for the development of biofunctional materials for the realization of innovative medicine.

Data Availability

The raw/processed data required to reproduce these findings cannot be shared at this time as the data also forms part of an ongoing study.

References

[1] D.A. Classen, The indications and reliability of vein graft use in free flap transfer, Can J Plast Surg 12(1) (2004) 27-9.

[2] M.C. Furr, S. Cannady, M.K. Wax, Interposition vein grafts in microvascular head and neck reconstruction, Laryngoscope 121(4) (2011) 707-11.

[3] J.A. Nelson, J.P. Fischer, R. Grover, S.J. Kovach, D.W. Low, S.K. Kanchwala, L.S. Levin, J.M. Serletti, L.C. Wu, Vein grafting your way out of trouble: Examining the utility and efficacy of vein grafts in microsurgery, J Plast Reconstr Aesthet Surg 68(6) (2015) 830-6.

[4] A. Meyer, K. Goller, R.E. Horch, J.P. Beier, C.D. Taeger, A. Arkudas, W. Lang, Results of combined vascular reconstruction and free flap transfer for limb salvage in patients with critical limb ischemia, J Vasc Surg 61(5) (2015) 1239-48.

[5] J.R. Harris, H. Seikaly, Evaluation of polytetrafluoroethylene micrografts in

microvascular surgery, J Otolaryngol 31(2) (2002) 89-92.
[6] T.Y. Shen, G.M. Mitchell, W.A. Morrison, B.M. O'Brien, The use of long synthetic microvascular grafts to vascularise free flaps in rabbits, Br J Plast Surg 41(3) (1988) 305-12.
[7] A.K. Kasabian, P.M. Glat, Y. Eidelman, N. Karp, G. Giangola, Limb salvage with microvascular free flap reconstruction using simultaneous polytetrafluoroethylene graft for inflow, Ann Plast Surg 35(3) (1995) 310-5.
[8] J.D. Cohn, K.F. Korver, Selection of saphenous vein conduit in varicose vein disease, Ann Thorac Surg 81(4) (2006) 1269-74.
[9] D.G. Seifu, A. Purnama, K. Mequanint, D. Mantovani, Small-diameter vascular tissue engineering, Nat Rev Cardiol 10(7) (2013) 410-21.
[10] S. Pashneh-Tala, S. MacNeil, F. Claeyssens, The Tissue-Engineered Vascular Graft-Past, Present, and Future, Tissue Eng Part B-Re 22(1) (2016) 68-100.
[11] W.E. Burkel, D.W. Vinter, J.W. Ford, R.H. Kahn, L.M. Graham, J.C. Stanley, Sequential studies of healing in endothelial seeded vascular prostheses: histologic and ultrastructure characteristics of graft incorporation, J Surg Res 30(4) (1981) 305-24.
[12] J.G. Ganske, R.J. Demuth, S.H. Miller, D.C. Buck, J.L. Dolph, Comparison of expanded polytetrafluoroethylene microvascular grafts to autogenous vein grafts, Plast Reconstr Surg 70(2) (1982) 193-201.
[13] S.W. Barttelbort, M.J. O'Leary, J. Schneider, W. Woodruff, Rat epigastric pedicle model: a clinically relevant evaluation of 1-mm PTFE grafts, Microsurgery 6(4) (1985) 233-6.
[14] V. Paloma, J.M. Lasso, A. Bazan, J.M. Serra, Relationship between flow and incidence of thrombosis in polytetrafluoroethylene vascular grafts in free microvascular flaps in lambs, Scand J Plast Reconstr Surg Hand Surg 33(3) (1999) 287-94.
[15] M.T.C. Wong, J. Lim, L.T. Chye, Use of stretch expanded polytetrafluoroethylene as a microvascular graft in a low-pressure situation, Asian J Surg 30(3) (2007) 188-192.
[16] P.K. Maitz, M. Lanzetta, E.R. Owen, Free-flap transfer with a synthetic arterial pedicle, J Reconstr Microsurg 15(3) (1999) 177-81.

[17] M.A. Cleary, E. Geiger, C. Grady, C. Best, Y. Naito, C. Breuer, Vascular tissue engineering: the next generation, Trends Mol Med 18(7) (2012) 394-404.
[18] R.L. Madden, G.S. Lipkowitz, B.J. Browne, A. Kurbanov, Experience with cryopreserved cadaveric femoral vein allografts used for hemodialysis access, Ann Vasc Surg 18(4) (2004) 453-8.
[19] S.S. Wang, S.H. Chu, Clinical use of omniflow vascular graft as arteriovenous bridging graft for hemodialysis, Artif Organs 20(12) (1996) 1278-81.
[20] H. Peng, E.M. Schlaich, S. Row, S.T. Andreadis, D.D. Swartz, A novel ovine ex vivo arteriovenous shunt model to test vascular implantability, Cells Tissues Organs 195(1-2) (2012) 108-21.
[21] A. Mahara, S. Somekawa, N. Kobayashi, Y. Hirano, Y. Kimura, T. Fujisato, T. Yamaoka, Tissue-engineered acellular small diameter long-bypass grafts with neointima-inducing activity, Biomaterials 58 (2015) 54-62.
[22] M.F. Cutiongco, M. Kukumberg, J.L. Peneyra, M.S. Yeo, J.Y. Yao, A.J. Rufaihah, C. Le Visage, J.P. Ho, E.K. Yim, Submillimeter Diameter Poly(Vinyl Alcohol) Vascular Graft Patency in Rabbit Model, Front Bioeng Biotechnol 4 (2016) 44.
[23] F. Kuwabara, Y. Narita, A. Yamawaki-Ogata, M. Satake, H. Kaneko, H. Oshima, A. Usui, Y. Ueda, Long-term results of tissue-engineered small-caliber vascular grafts in a rat carotid arterial replacement model, J Artif Organs 15(4) (2012) 399-405.
[24] T. Fujisato, K. Minatoya, S. Yamazaki, Y. Meng, K. Niwaya, A. Kishida, T. Nakatani, S. Kitamura, Cardiovascular regeneration therapies using tissue engineering approaches, Springer, Tokyo. (2005) 83-94.
[25] S. Funamoto, K. Nam, T. Kimura, A. Murakoshi, Y. Hashimoto, K. Niwaya, S. Kitamura, T. Fujisato, A. Kishida, The use of high-hydrostatic pressure treatment to decellularize blood vessels, Biomaterials 31(13) (2010) 3590-5.
[26] A.Y. Wang, X. Mo, C.S. Chen, S.M. Yu, Facile modification of collagen directed by collagen mimetic peptides, J Am Chem Soc 127(12) (2005) 4130-1.
[27] B. Strauch, D.E. Murray, Transfer of composite graft with immediate suture anastomosis of its vascular pedicle measuring less than 1 mm. in external diameter using microsurgical techniques, Plast Reconstr Surg 40(4) (1967)

325-9.
[28] T. Mucke, A. Borgmann, S. Wagenpfeil, R. Gunzinger, C. Nobauer, R. Lange, J. Slotta-Huspenina, F. Holzle, K.D. Wolff, Autonomization of epigastric flaps in rats, Microsurgery 31(6) (2011) 472-8.
[29] P.M. Crapo, T.W. Gilbert, S.F. Badylak, An overview of tissue and whole organ decellularization processes, Biomaterials 32(12) (2011) 3233-3243.
[30] T. Ehashi, A. Nishigaito, T. Fujisato, Y. Moritan, T. Yamaoka, Peripheral Nerve Regeneration and Electrophysiological Recovery with CIP-Treated Allogeneic Acellular Nerves, J Biomat Sci-Polym E 22(4-6) (2011) 627-640.
[31] M. Hirata, T. Yamaoka, Hepatocytic differentiation of iPS cells on decellularized liver tissue, J Artif Organs (2017).
[32] T.J. Keane, I.T. Swinehart, S.F. Badylak, Methods of tissue decellularization used for preparation of biologic scaffolds and in vivo relevance, Methods 84 (2015) 25-34.
[33] H.G. Butler, 3rd, L.D. Baker, Jr., J.M. Johnson, Vascular access for chronic hemodialysis: polytetrafluoroethylene (PTFE) versus bovine heterograft, Am J Surg 134(6) (1977) 791-3.
[34] H.E. Katzman, M.H. Glickman, A.F. Schild, R.M. Fujitani, J.H. Lawson, Multicenter evaluation of the bovine mesenteric vein bioprostheses for hemodialysis access in patients with an earlier failed prosthetic graft, J Am Coll Surg 201(2) (2005) 223-30.
[35] E.S. Chemla, M. Morsy, Randomized clinical trial comparing decellularized bovine ureter with expanded polytetrafluoroethylene for vascular access, Br J Surg 96(1) (2009) 34-9.
[36] G.E. Sandusky, G.C. Lantz, S.F. Badylak, Healing comparison of small intestine submucosa and ePTFE grafts in the canine carotid artery, J Surg Res 58(4) (1995) 415-20.
[37] X. Mo, Y.J. An, C.S. Yun, S.M. Yu, Nanoparticle-assisted visualization of binding interactions between collagen mimetic peptide and collagen fibers, Angew Chem Int Edit 45(14) (2006) 2267-2270.
[38] A.Y. Wang, C.A. Foss, S. Leong, X. Mo, M.G. Pomper, S.M. Yu, Spatio-temporal modification of collagen scaffolds mediated by triple helical propensity, Biomacromolecules 9(7) (2008) 1755-1763.

[39] C.A. Miles, M. Ghelashvili, Polymer-in-a-box mechanism for the thermal stabilization of collagen molecules in fibers, Biophys J 76(6) (1999) 3243-3252.
[40] W.M. Abbott, J. Megerman, J.E. Hasson, G. L'Italien, D.F. Warnock, Effect of compliance mismatch on vascular graft patency, J Vasc Surg 5(2) (1987) 376-82.
[41] T. Mizuno, T. Tsukiya, Y. Takewa, E. Tatsumi, Differences in clotting parameters between species for preclinical large animal studies of cardiovascular devices, J Artif Organs (2017).

Table Legend

Table 1. Graft patency and survival of the epigastric flaps.

Figure Legend

Fig. 1. Rat tail artery before (A) and after (B and C) decellularization. Inner diameter and length of the grafts were 0.6 mm and 7 cm respectively (C). The arrows indicate the dorsal branch of the tail artery.

Fig. 2. (A) Schematic diagram of the rat epigastric flap model. (B) Laser speckle images of the flaps with intact pedicles (a) and those with pedicles ligated and cut at the arrowed position (b). The flap survival depended on blood flow from the pedicle.

Fig. 3. Schematic diagram of the graft transplantation between the right femoral artery and the pedicle of the epigastric flap. The arrows indicate the graft with 5 cm length.

Fig. 4. Analysis of decellularization. (A) H&E staining of the decellularized grafts prepared by UHP (above) and SDS treatment (below). (B) DNA contents in native arteries and decellularized grafts (n=3).

Fig.5. Evaluation of functionalized lumen of decellularized graft in each group. (A) SEM images of the graft lumen in each group and that of the native artery as a control. (B) Confocal microscopy images of the graft lumen of each group modified with labeled peptide - before perfusion (left) and after perfusion (right).

Fig. 6. Relation between pressure and diameter in the decellularized grafts.

Fig. 7. Histological evaluation of the grafts after 3 weeks of transplantation.
(A) Evaluation of re-endothelialization with CD31 immunostains. CD31 positive cell layer formation was observed in UHP-37 (above), and not in UHP-4 (below). The dotted lines indicate the suture lines. The arrows indicate outgrowth of the endothelial cells from the native artery, while asterisks indicate inside of the graft.
(B) H&E staining of an example of the dissecting aneurysms. The black arrow indicates the internal elastic lamina and the white arrow indicates the tunica media.

Supplemental Figure S1. Gross appearance and laser-speckle image of each flap at the last observation. The dotted square indicates flap area. Only one flap showed total necrosis (arrows).

Supplemental Figure S2. Representative gross appearance of the UHP-60 group. Thrombus formation was seen across the whole area except the anastomosis.

Supplemental Figure S3. Ultrasound Doppler image (A) and gross appearance (B) at 3 weeks of the representative patent graft of the UHP-37 group. Laser speckle image also demonstrated the graft patency (B, below). White arrows indicate the vascular graft. Black arrows indicate the epigastric flap.

Table 1. Graft patency and survival of the epigastric flaps.

Group	Graft patency			Flap survival
	Day 1	Day 7	Day 21	
UHP-60	6/6	6/6	0/6	6/6
UHP-37	6/6	6/6	6/6	6/6
UHP-4	3/3	2/3	2/3	3/3
SDS-37	2/3	2/3	0/3	2/3

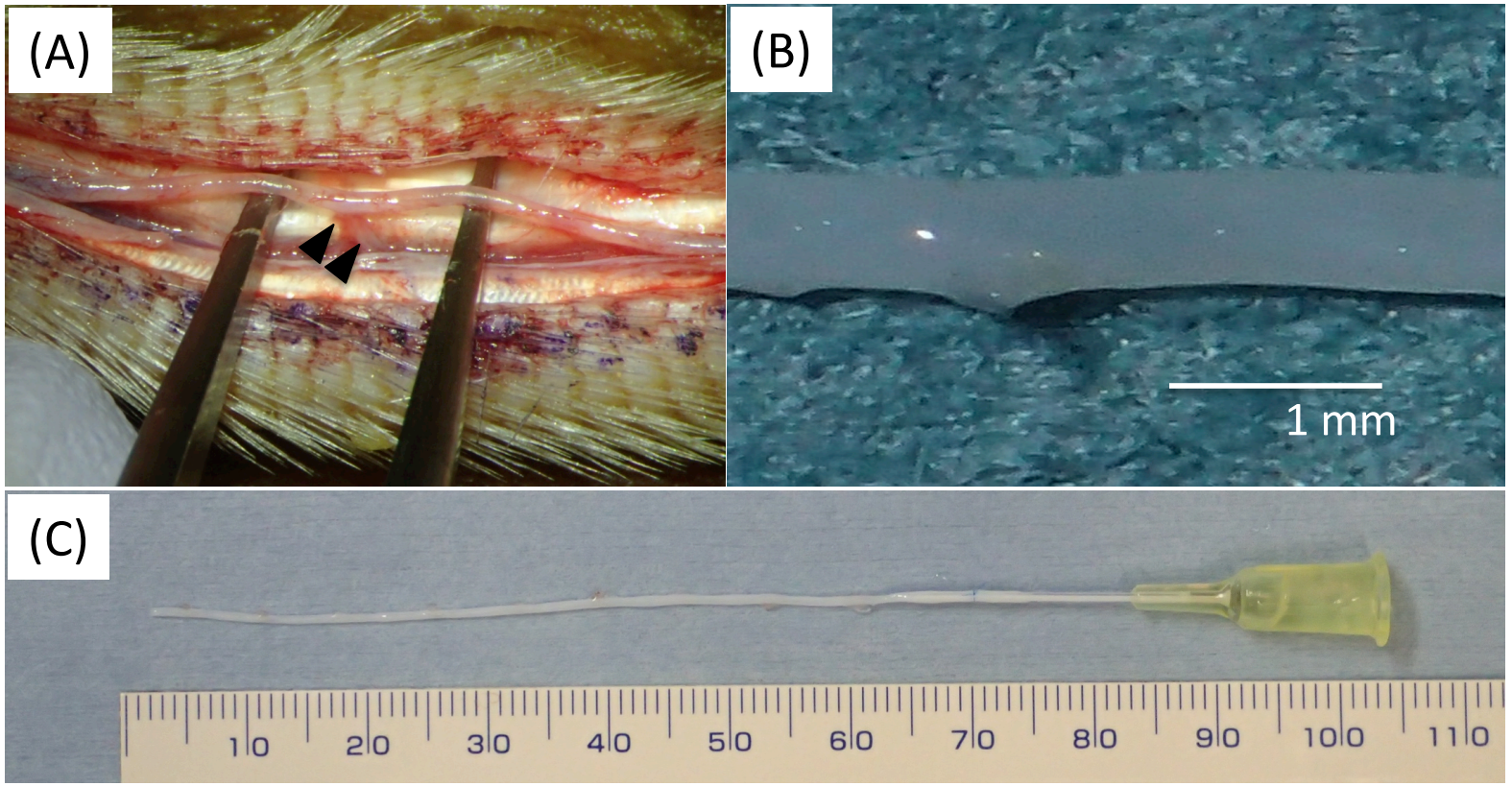

Fig. 1. Rat tail artery before (A) and after (B and C) decellularization. Inner diameter and length of the grafts were 0.6 mm and 7 cm respectively (C). The arrows indicate the dorsal branch of the tail artery.

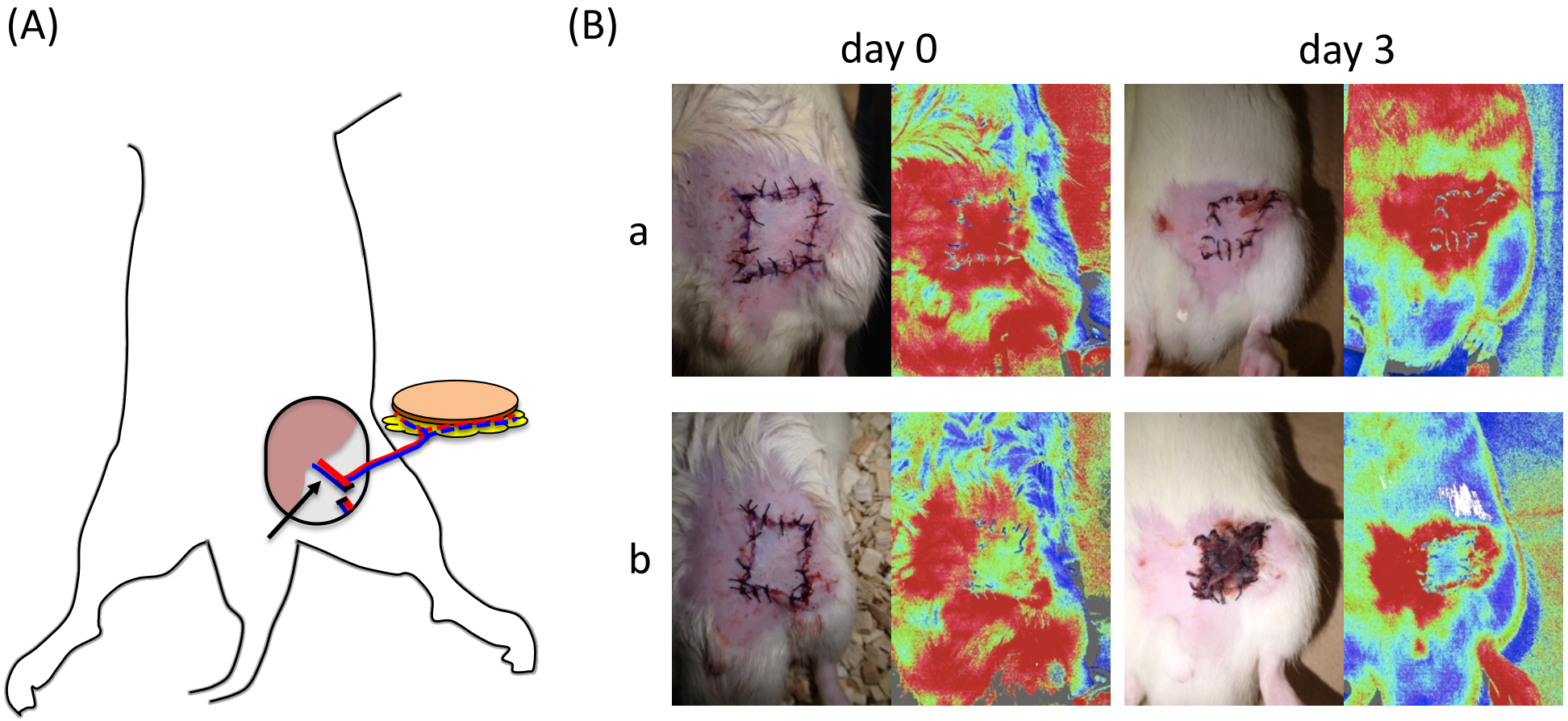

Fig. 2. (A) Schematic diagram of the rat epigastric flap model. (B) Laser speckle images of the flaps with int
pedicles (a) and those with pedicles ligated and cut at the arrowed position (b). The flap survival dependec
on blood flow from the pedicle.

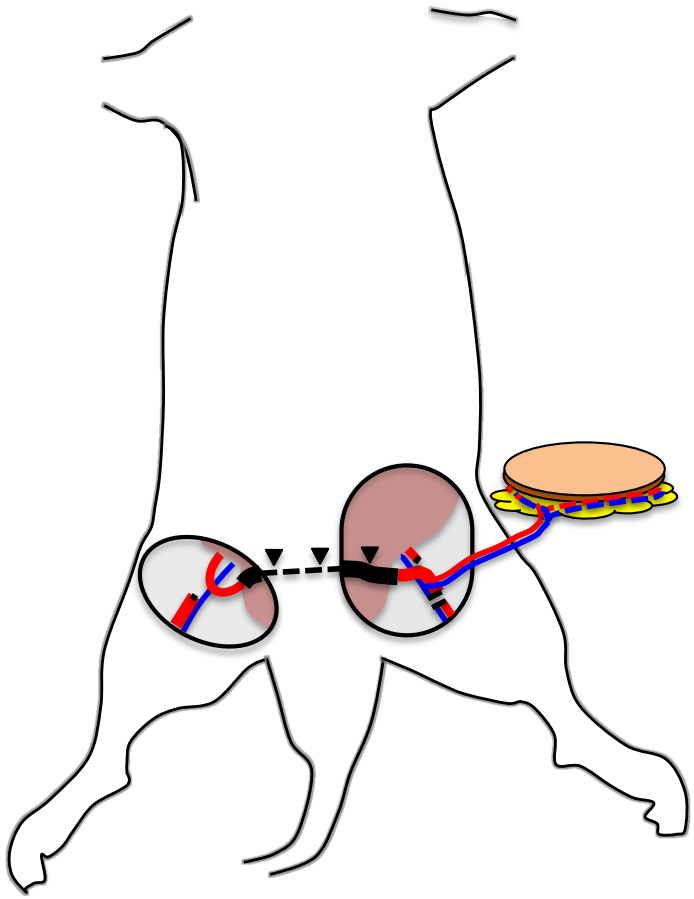

Fig. 3. Schematic diagram of the graft transplantation between the right femoral artery and the pedicle of the epigastric flap. The arrows indicate the graft with 5 cm length.

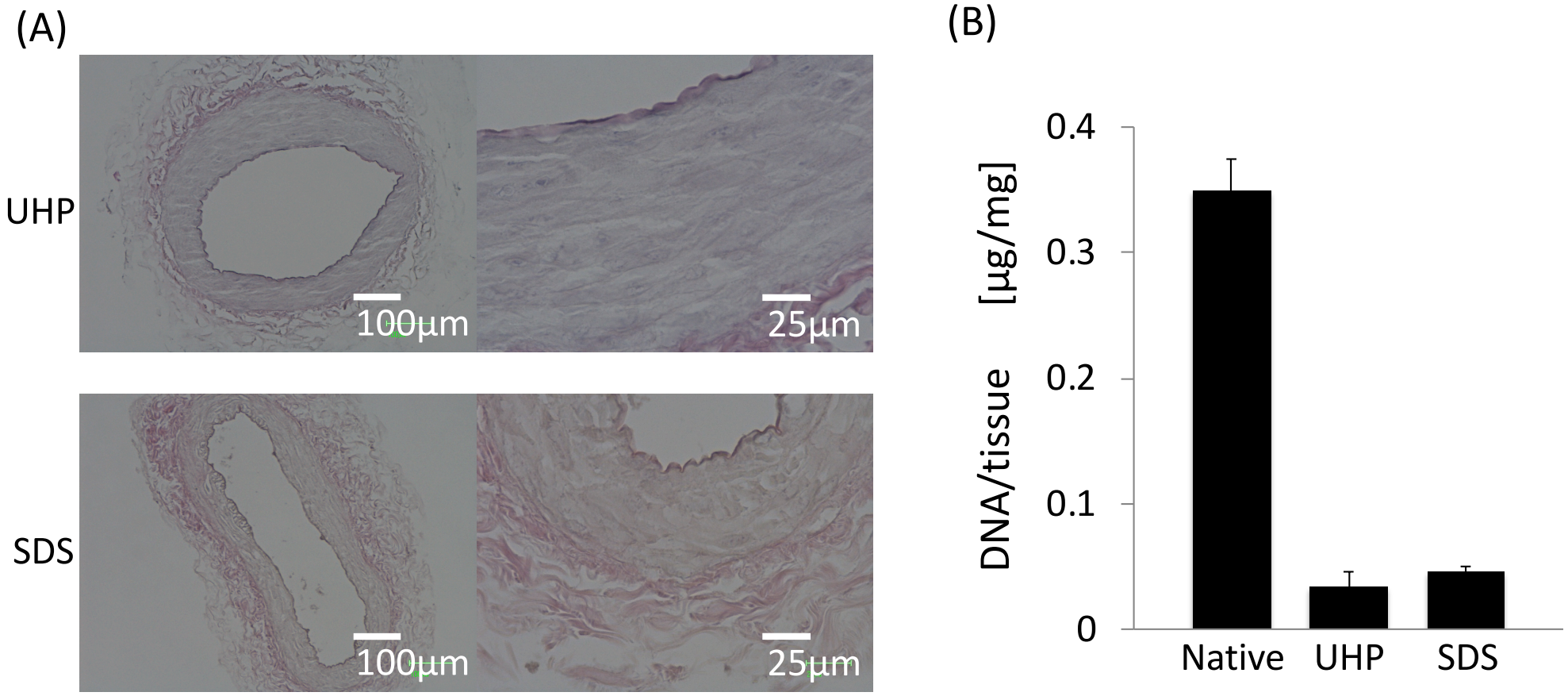

Fig. 4. Analysis of decellularization. (A) H&E staining of the decellularized grafts prepared by UHP (above) and SDS treatment (below). (B) DNA contents in native arteries and decellularized grafts (n=3).

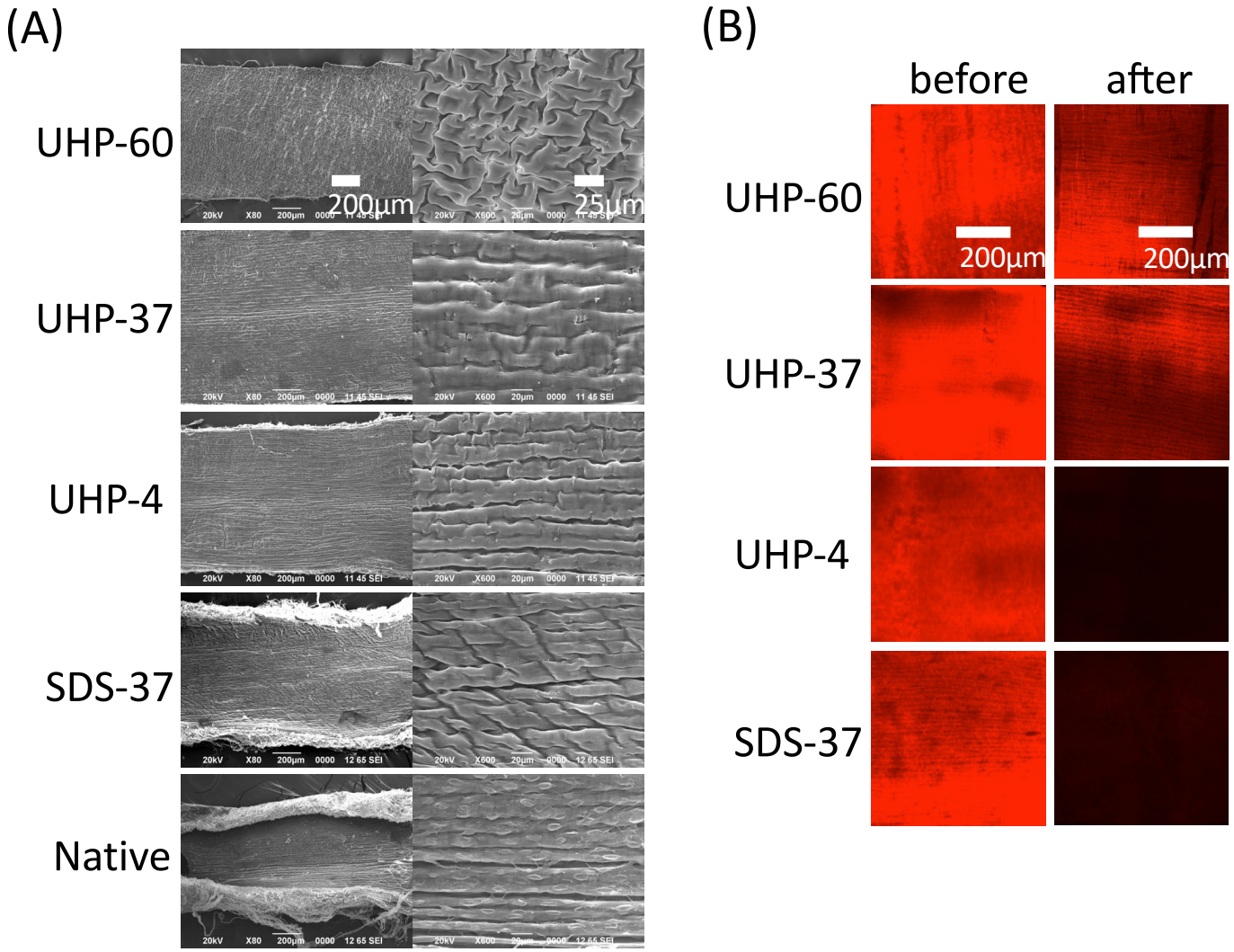

Fig.5. Evaluation of functionalized lumen of decellularized graft in each group.
(A) SEM images of the graft lumen in each group and that of the native artery as a control.
(B) Confocal microscopy images of the graft lumen of each group modified with labeled peptide - before perfusion (left) and after perfusion (right).

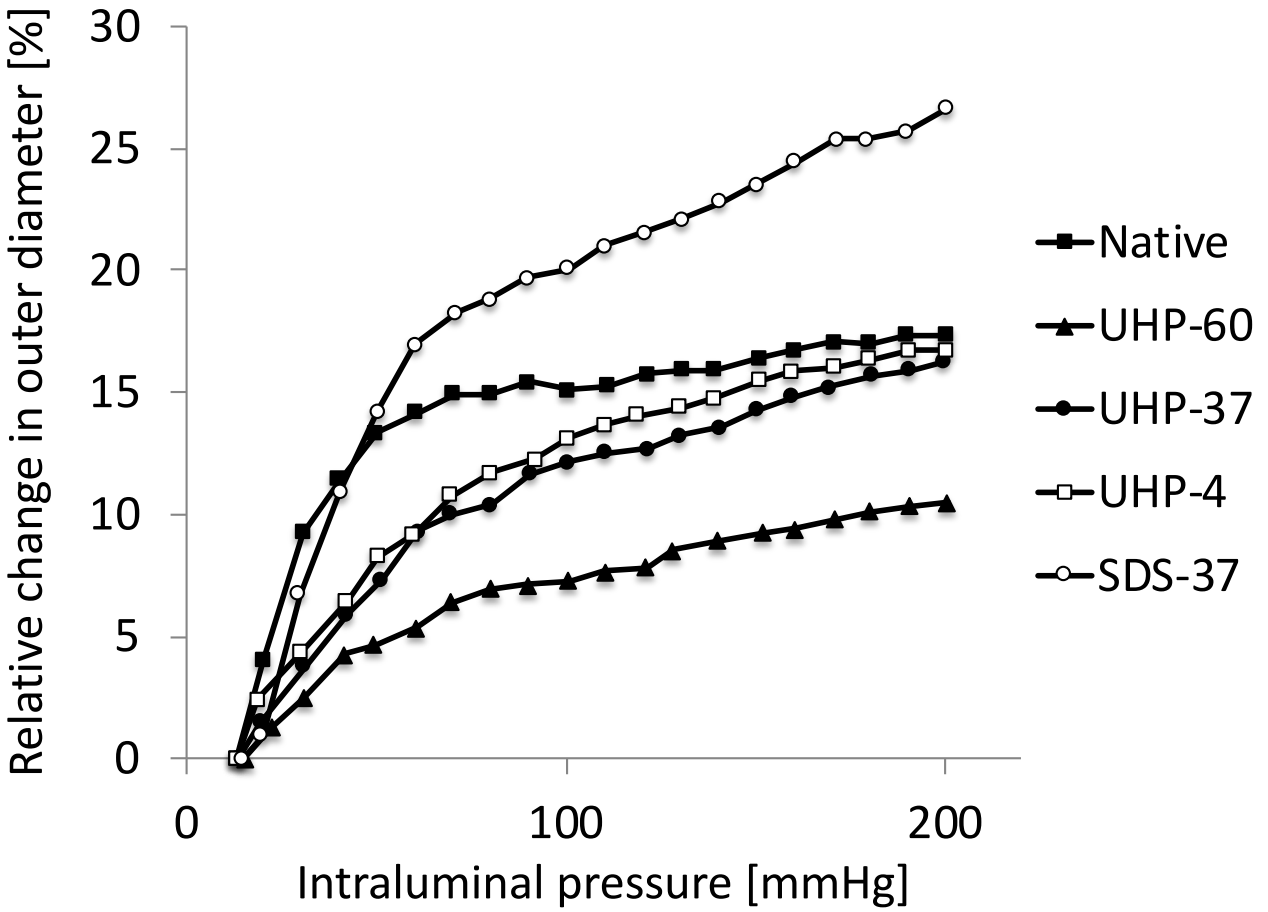

Fig. 6. Relation between pressure and diameter in the decellularized grafts.

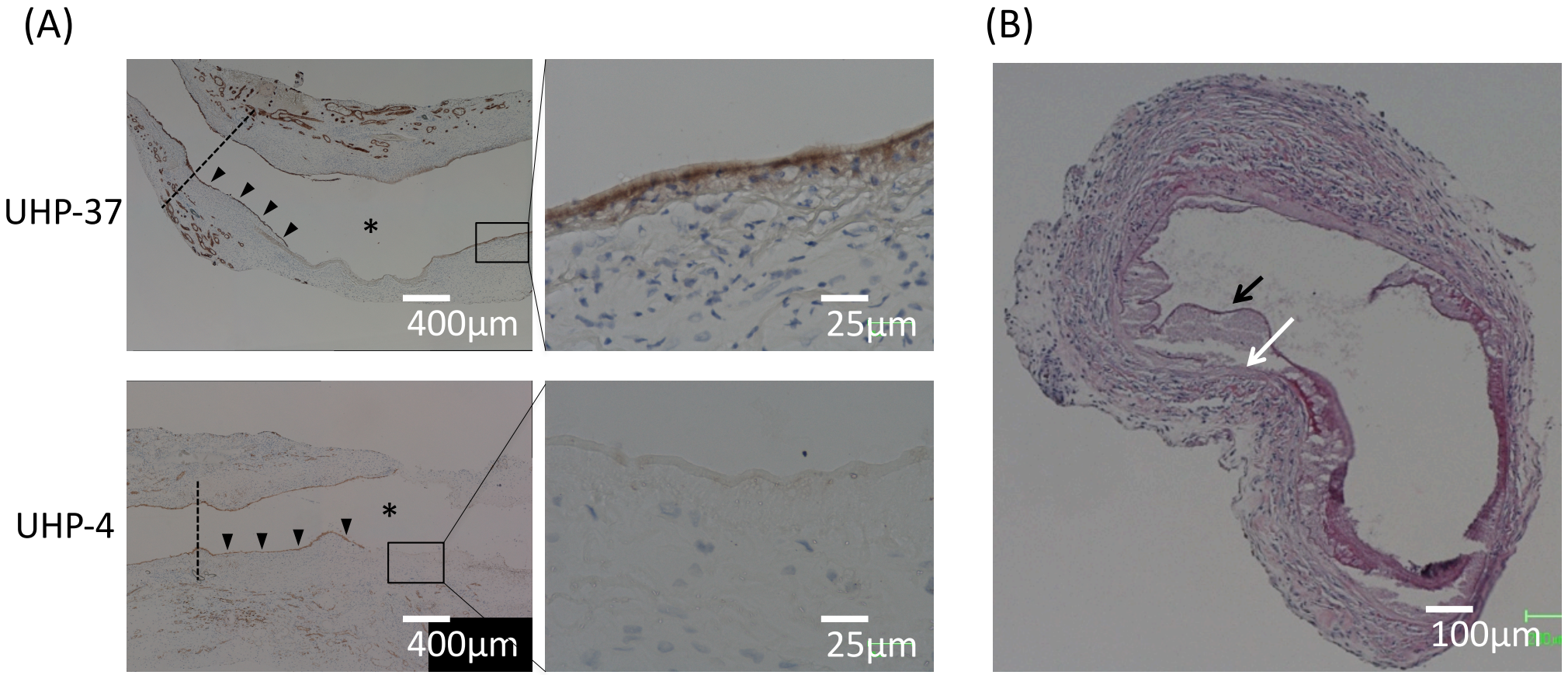

Fig. 7. Histological evaluation of the grafts after 3 weeks of transplantation.
(A) Evaluation of re-endothelialization with CD31 immunostains. CD31 positive cell layer formation was observed in UHP-37 (above), and not in UHP-4 (below). The dotted lines indicate the suture lines. The arrows indicate outgrowth of the endothelial cells from the native artery, while asterisks indicate inside of the graft. (B) H&E staining of an example of the dissecting aneurysms. The black arrow indicates the internal elastic lamina and the white arrow indicates the tunica media.

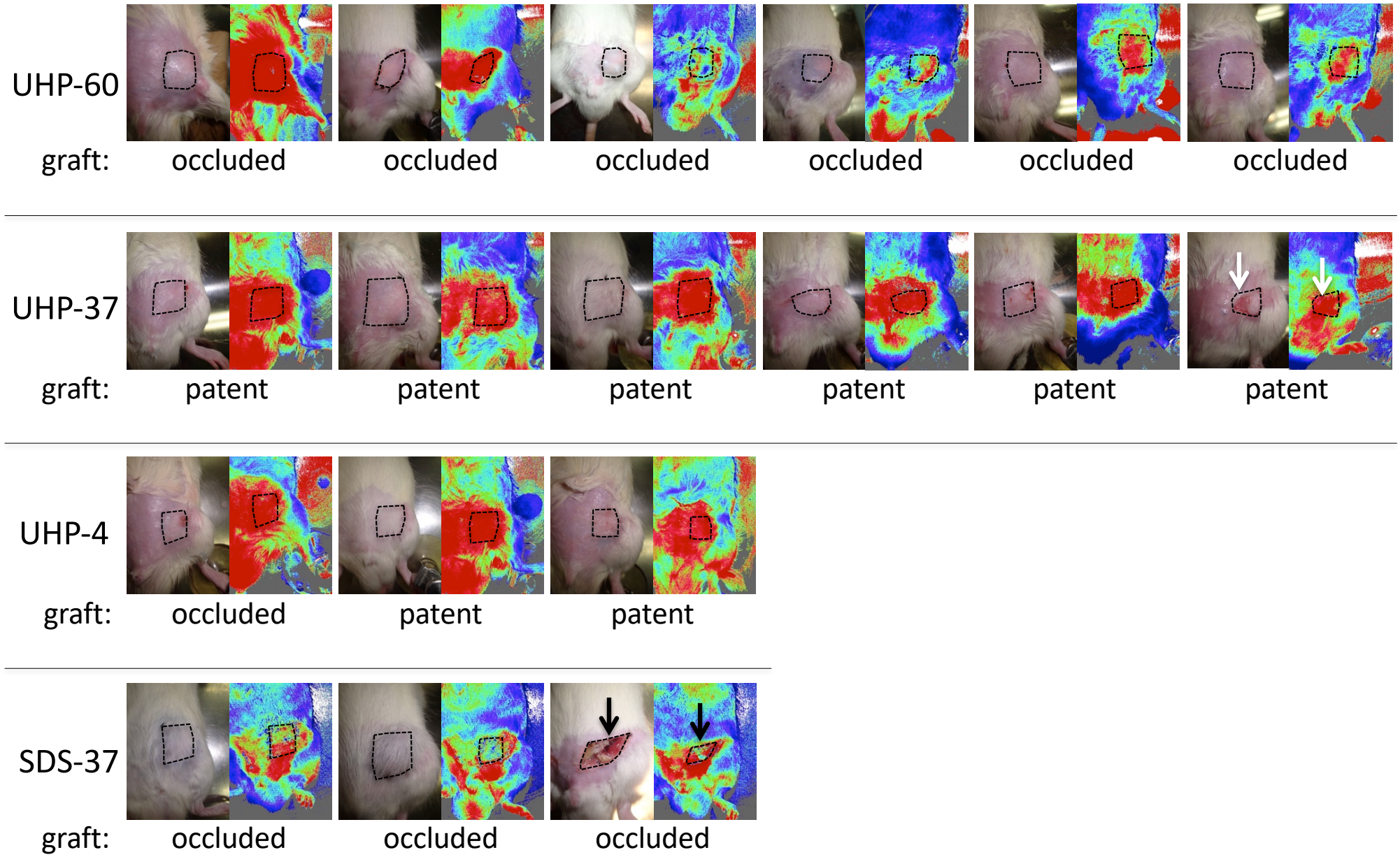

Supplemental Figure S1. Gross appearance and laser-speckle image of each flap at the last observation. The dotted square indicates flap area. Only one flap showed total necrosis (black arrows). One of UHP-37 showed ulceration due to self-mutilation (white arrows).

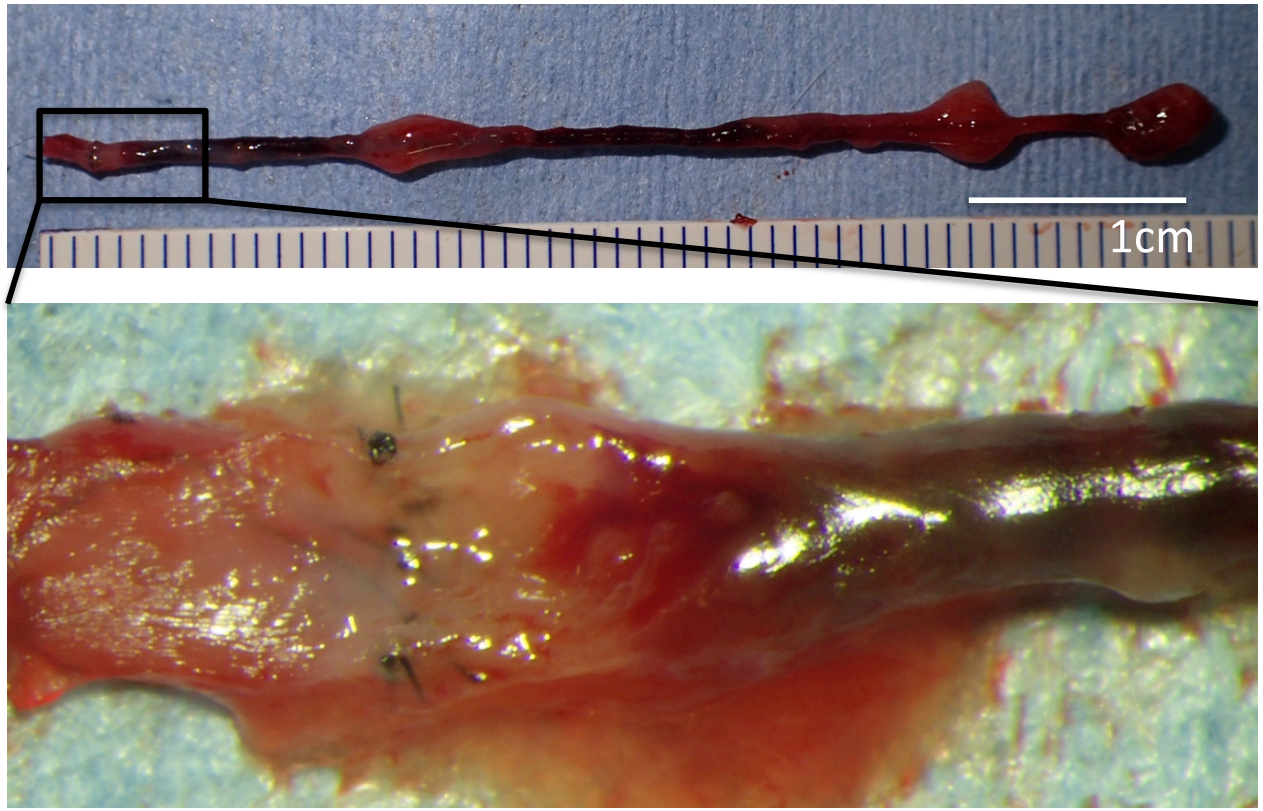

Supplemental Figure S2. Representative gross appearance of the UHP-60 group. Thrombus formation was seen across the whole area except the anastomosis.

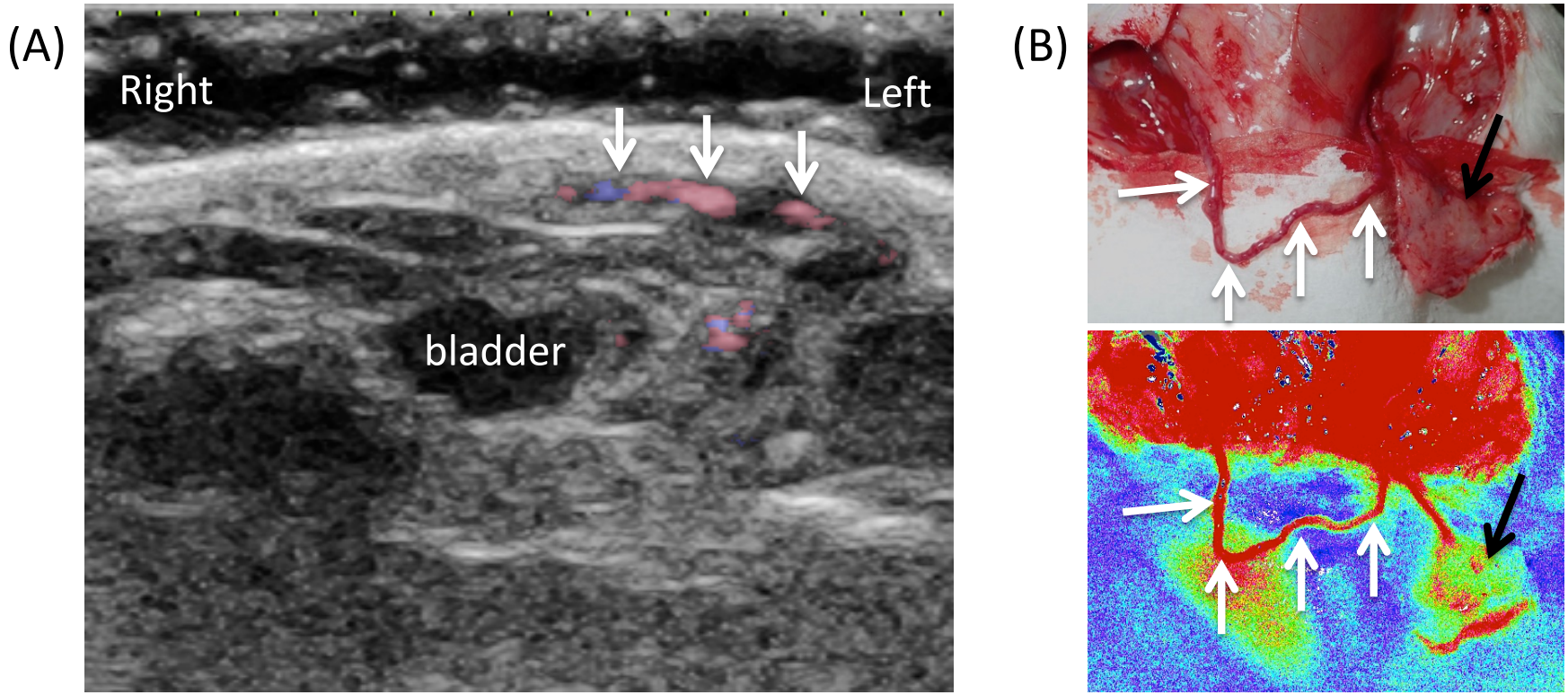

Supplemental Figure S3. Ultrasound Doppler image (A) and gross appearance (B) at 3 weeks of the representative patent graft of the UHP-37 group. Laser speckle image also demonstrated the graft patency (B, below). White arrows indicate the vascular graft. Black arrows indicate the epigastric flap.